Simultaneous Removal of NO_x and Mercury in Low Temperature Selective Catalytic and Adsorptive Reactor

Final Scientific Report

September 1, 2004 to February 28, 2006

Dr. Neville G. Pinto (PI)
Dr. Panagiotis (Peter) G. Smirniotis (co-PI)

August, 2006

DOE Grant No. DE-FG26-04NT42180

Department of Chemical & Materials Engineering
P.O. Box 210012
University of Cincinnati
Cincinnati, OH 45221-0012

Disclaimer

ABSTRACT

The results of a 18-month investigation to advance the development of a novel Low Temperature Selective Catalytic and Adsorptive Reactor (LTSCAR), for the simultaneous removal of NO_x and mercury (elemental and oxidized) from flue gases in a single unit operation located downstream of the particulate collectors, are reported. In the proposed LTSCAR, NO_x removal is in a traditional SCR mode but at low temperature, and, uniquely, using carbon monoxide as a reductant. The concomitant capture of mercury in the unit is achieved through the incorporation of a novel chelating adsorbent. As conceptualized, the LTSCAR will be located downstream of the particulate collectors (flue gas temperature 140-160^oC) and will be similar in structure to a conventional SCR. That is, it will have 3-4 beds that are loaded with catalyst and adsorbent allowing staged replacement of catalyst and adsorbent as required.

Various Mn/TiO_2 SCR catalysts were synthesized and evaluated for their ability to reduce NO at low temperature using CO as the reductant. It has been shown that with a suitably tailored catalyst more than 65 % NO conversion with 100% N_2 selectivity can be achieved, even at a high space velocity (SV) of 50,000 h^{-1} and in the presence of 2 v% H_2O.

Three adsorbents for oxidized mercury were developed in this project with thermal stability in the required range. Based on detailed evaluations of their characteristics, the mercaptopropyltrimethoxysilane (MPTS) adsorbent was found to be most promising for the capture of oxidized mercury. This adsorbent has been shown to be thermally stable to 200^oC. Fixed-bed evaluations in the targeted temperature range demonstrated effective removal of oxidized mercury from simulated flue gas at very high capacity (>≈58 mg Hg/g adsorbent).

Extension of the capability of the adsorbent to elemental mercury capture was pursued with two independent approaches: incorporation of a novel nano-layer on the surface of the chelating mercury adsorbent to achieve *in situ* oxidation on the adsorbent, and the use of a separate titania-supported manganese oxide catalyst upstream of the oxidized mercury adsorbent. Both approaches met with some success. It was demonstrated that the concept of *in situ* oxidation on the adsorbent is viable, but the future challenge is to raise the operating capacity beyond the achieved limit of 2.7 mg Hg/g adsorbent. With regard to the manganese dioxide catalyst, elemental mercury was very efficiently oxidized in the absence of sulfur dioxide. Adequate resistance to sulfur dioxide must be incorporated for the approach to be feasible in flue gas.

A preliminary benefits analysis of the technology suggests significant potential economic and environmental advantages.

TABLE OF CONTENTS

Section			Page
	EXECUTIVE SUMMARY		**4**
I.	**Introduction**		**6**
II.	**Experimental Methods**		**7**
	A.	**Catalyst Preparation**	**7**
	B.	**Catalyst Characterization**	**7**
	C.	**Adsorbent Synthesis**	**8**
	D.	**Adsorbent Characterization**	**9**
		Surface Area and Pore Size Distribution	**9**
		Elemental Analysis	**9**
		Thermo-Gravimetric Analysis (TGA)	**9**
	E.	**Packed-Bed Evaluations**	**10**
		Nitrogen Oxide Reduction	**10**
		Mercury Adsorption	**11**
III.	**Results and Discussion**		**12**
	A.	**Low Temperature NO_x Reduction with CO**	**12**
	B.	**Oxidation of Elemental Mercury**	**16**
		Modification of Chelating Adsorbent	**16**
		Titania Supported Hg(0) Oxidizing Catalyst	**18**
	C.	**Thermally Robust Adsorbents for Oxidized Mercury**	**21**
		MPTS Adsorbent	**21**
		CPTS-DZ Adsorbent	**22**
		APTS-MBT Adsorbent	**24**
		Operating Capacity Evaluations	**27**
IV.	**Preliminary Assessment of Economic Impact**		**29**
V.	**Conclusions**		**32**
VI.	**References**		**33**

EXECUTIVE SUMMARY

An 18-month investigation to advance the development of a novel Low Temperature Selective Catalytic and Adsorptive Reactor (LTSCAR) for the simultaneous removal of NO_x and mercury (elemental and oxidized) from flue gases in a single unit operation located downstream of the particulate collectors has been completed. The work was based on two previous developments at the University of Cincinnati: (1) the synthesis of promising TiO_2 based transition metal catalysts for low temperature NO_x reduction; and (2) the development of a novel high-capacity chelating agent for vapor-phase mercury capture. The overall goal of this project was to explore the feasibility of the LTSCAR concept, where NO_x removal is to be achieved in a traditional SCR mode but at low temperature, and, uniquely, using carbon monoxide as a reductant, to circumvent the existing challenges with ammonia. The concomitant capture of mercury in the unit is targeted, through the incorporation of a recently developed chelating adsorbent. As conceptualized, the LTSCAR will be located downstream of the particulate collectors (flue gas temperature 140-160^oC) and will be similar in structure to a conventional SCR. That is, it will have 3-4 beds that are loaded with catalyst and adsorbent allowing staged replacement of catalyst and adsorbent as required.

This preliminary, fundamental investigation of the feasibility of the LTSCAR involved the following specific technical objectives: (1) Development of a Mn/TiO_2 SCR catalyst that uses CO as the reductant and is effective below 180^oC; (2) Incorporation of Mn sites on the catalyst to oxidize elemental mercury; (3) Synthesis of a chelating adsorbent that is stable up to 200^oC; and (4) Modification of the chelating adsorbent to incorporate *in situ* oxidation of elemental mercury.

Various Mn/TiO_2 SCR catalysts were synthesized and evaluated for their ability to reduce NO at low temperature using CO as the reductant. It has been shown that with proper selection of catalyst more than 65 % NO conversion with 100% N_2 selectivity can be achieved, even at a high space velocity (SV) of 50,000 h^{-1} and in the presence of 2 v% H_2O. It is postulated, based on the results of this study, that moderate surface acidity, a high surface manganese oxide concentration, and redox properties of the catalyst are important factors in achieving better DeNOx performance at low temperature.

The development of an LTSCAR adsorbent for mercury involved two challenges: raising the allowable temperature of operation of the available prototype to a minimum of 160^oC, and extending the sorbent capability to include elemental mercury in addition to oxidized mercury. Three adsorbents were developed in this project with thermal stability in the required range. Based on detailed evaluations of their characteristics, the mercaptopropyltrimethoxysilane (MPTS) adsorbent was identified as most promising for oxidized mercury. This adsorbent has been shown to be thermally stable to 200^oC. Fixed-bed evaluations in the targeted temperature range demonstrated effective removal of oxidized mercury from simulated flue gases at very high capacity (>≈58 mg Hg/g adsorbent).

Extension of the capability of the adsorbent to elemental mercury capture is essential to ensure that the performance of the LTSCAR is independent of coal type, combustion conditions, plant configuration, etc. Two independent approaches were explored: incorporation of a novel nano-layer on the surface of the chelating mercury adsorbent to achieve *in situ* oxidation on the adsorbent, and the use of a separate titania-supported manganese oxide catalyst upstream of the oxidized mercury adsorbent. In both cases the objective was to oxidize elemental mercury prior to capture by chelation on the adsorbent, and each met with some success. It was demonstrated that the concept of *in situ* oxidation on the adsorbent is viable, but the future challenge is to raise the operating capacity beyond the achieved limit of 2.7 mg Hg/g adsorbent. With regard to the manganese dioxide catalyst, elemental mercury was very efficiently oxidized in the absence of sulfur dioxide. Adequate resistance to sulfur dioxide must be incorporated for the approach to be feasible in flue gas. Research is currently underway in Phase II of this project to overcome the limitations discovered.

Though a benefit analysis of LTSCAR based on the results of this project is necessarily preliminary, significant advantages are expected. Low temperature SCR catalysts offer the opportunity to remove NO_x without the need to reheat the flue gas stream, with obvious economic benefits. The use of CO as a reductant, if proven successful, will replace the current reductants for medium and low temperature SCR, namely ammonia and/or urea, an upgrade for the industry. It will eliminate the need to buy reductants and transport them to the site, minimize equipment corrosion, and eliminate storage of reductants. Also, the operating cost can be expected to decrease significantly. The incorporation of concomitant mercury removal in the SCR unit has the potential for reducing the total cost of environmental compliance, and incorporates the significant advantage of a smaller retrofit imprint for existing plants. Additionally the availability of a high capacity, selective adsorbent with strong binding energy for mercury has the added advantages of reducing secondary waste and providing tighter control on the ultimate fate of the captured mercury. However, the greatest potential benefit appears to be in the much lower cost for capture, which is expected to be a factor of 10 lower than for available technologies.

I. Introduction

An 18-month investigation to advance the development of a novel, advanced Low Temperature Selective Catalytic and Adsorptive Reactor (LTSCAR) for the simultaneous removal of NO_x and mercury (elemental and oxidized) from flue gases in a single unit operation, located downstream of the particulate collectors (Figure 1) has been completed. The work was based on two previous developments at the University of Cincinnati: (1) the synthesis of promising TiO_2 based transition metal catalysts for low temperature NO_x reduction; and (2) the development of a novel high-capacity chelating agent for vapor-phase mercury capture. The goal of the project was to investigate adapting these technologies into an integrated removal process for both pollutants. To achieve this goal, the following specific technical objectives were pursued: (1) Development of a Mn/TiO_2 SCR catalyst that uses CO as the reductant and is effective below 180°C; (2) Incorporation of Mn sites on the catalyst to oxidize elemental mercury; (3) Synthesis of a chelating adsorbent that is stable up to 200°C; and (4) Modification of the chelating adsorbent to incorporate *in situ* oxidation of elemental mercury.

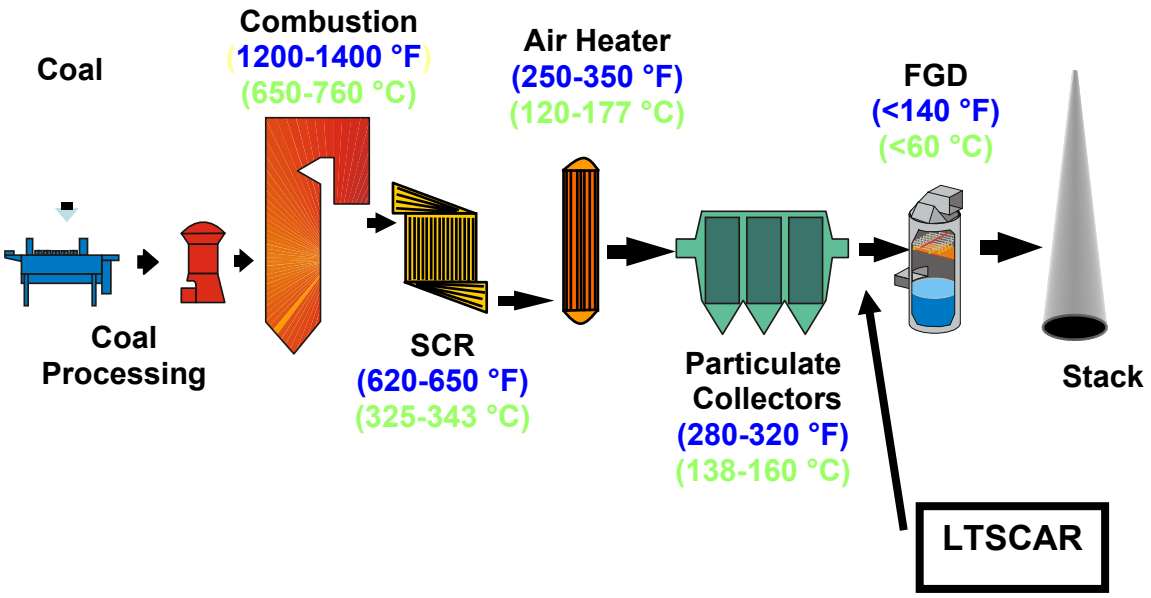

Figure 1. Location of Proposed LTSCAR in Flue Gas Train of Coal-Fired Power Plant

II. Experimental Methods

A. Catalyst Preparation

A series of high surface area anatase titania supported manganese oxide catalysts were prepared by a wet impregnation method. Commercially available Hombikat TiO_2 (Sachtleben Chemie, 99% anatase) was used as received. Manganese oxide was deposited by the solution impregnation method on the support, using aqueous solutions of manganese nitrate. In a typical synthesis, 50 ml of deionzied water was added to a 100 ml beaker containing 1 g of support. The mixture was heated to 343 K under continuous stirring. A measured quantity of nitrate precursor was then added to the solution, and the mixture was evaporated to dryness. The paste obtained was further dried overnight at 383 K. Catalysts were calcined at 673 K for 2 hours in a flow of O_2 (4.0% oxygen in helium).

B. Catalyst Characterization

X-ray powder diffraction patterns were recorded on a Siemens D500 diffractometer using a Cu K_α radiation source (wavelength 1.5406 Å). An aluminum holder was used to support the catalyst samples. The scanning range was 5°-70° (2θ) with a step size of 0.05° and a step time of 1s/. The XRD phases present in the samples were identified with the help of JCPDS data files.

The specific surface areas of the samples were determined on a Micromeritics 2360 instrument by nitrogen physisorption at liquid nitrogen temperature (77 K) and by taking 0.162 nm^2 as the molecular area of the nitrogen molecule. Pore volume measurements were performed on a Micromeritics ASAP 2010 using N_2 adsorption at 77K. All samples were degassed at 523 K under vacuum before analysis.

The ammonia TPD experiments were performed on a Micromeritics 2910 instrument using 50 mg of catalyst. Prior to the experiments the catalysts were pretreated at 773 K for 1 h in a highly pure He (30 ml min^{-1}) stream. The furnace temperature was lowered to 373 K, and the samples were then treated with anhydrous NH_3 (4% in He) at a flow rate of 30 ml min^{-1} for 1 h. Physisorbed NH_3 was removed by flushing the catalyst with helium at 373 K for 3-5 hours before starting the TPD experiments. Experimental runs were recorded by heating the sample in helium (30 ml min^{-1}) from 373 K to 773 K at a linear heating rate of 5 K min^{-1}, and finally keeping the temperature constant at 773 K for 1 hour to ensure complete ammonia desorption.

The temperature-programmed reduction (H_2-TPR) experiments were carried out from 353–1223 K on a Micromeritics AutoChem 2910 instrument using 50 mg of calcined catalyst. Prior to the analysis catalysts were pretreated at 673 K for 2 h in ultra high pure helium (30 ml min^{-1}) stream. The TPR runs were carried out with a linear heating rate (10 ºC/min) in a flow of 4% H_2 in argon with a flow rate of 25 ml min^{-1}. The hydrogen consumption was measured quantitatively by a thermal conductivity detector.

C. Adsorbent Synthesis

We have previously developed a novel chelating adsorbent for the capture of mercury in flue gases. The synthesis, structure and performance of the prototype have been described in detail in our recent publication (Abu Daabes and Pinto, 2005). One limitation is that the prototype cannot operate at temperatures above 130^0C. For the integration of NO_x and Hg removal in one unit, the conceived Low Temperature Selective Catalytic and Adsorptive Reactor (LTSCAR), it is necessary to develop adsorbents with higher thermal stability, to match the operating temperature range for the catalytic reduction of NO_x. Thermal stability studies on the prototype have demonstrated that the chelating ligand (cysteine) disintegrates at temperatures above 130^0C. Thus the focus was on identifying alternate ligands, and on developing the chemistry for attaching them to the silica substrate.

Based on a review of the literature three chelating ligands were identified for the synthesis of thermally robust versions of the mercury adsorbent: mercaptopropyltrimethoxysilane (MPTS), Dithizone (DZ), and Mercaptobenzothiazole (MBT). It is expected that these ligands will be thermally stable to at least 160^0C. Synthesis procedures have been developed to link these chelating groups to the porous silica substrate. These procedures are described briefly for each ligand:

(a) Immobilization of mercaptopropyltrimethoxysilane (MPTS) on the silica surface was performed by reacting acid-washed silica gel with MPTS using dry toluene as a solvent. A Büchi rotary evaporator (Model R-205) with total reflux was used as the reaction apparatus, and the oil bath temperature was 110°C. The product was filtered and the unreacted MPTS was extracted using a Soxhlet apparatus. The product was then dried under vacuum at 105 °C and is referred to as MPTS.

(b) Dithizone was chemically bonded to silica gel as follows. First, 4 g of acid washed silica was suspended in 100 ml dry toluene and 10 ml 3-chloropropyltrimethoxysilane (CPTS) under argon at 110 ºC oil bath temperature and total reflux for 20 hours. The mixture was allowed to cool to room temperature before it was filtered. The solid product was transferred to a Soxhlet apparatus and was extracted with dry toluene, to remove the unreacted CPTS. The solid product was then removed and subjected to thermal curing under vacuum at 70 °C overnight. This intermediate product is called CPTS-Silica.

CPTS-Silica was then added to a solution of DZ dissolved in dry toluene in the presence of few drops of pyridine. The reaction mixture was refluxed for about 22 hours at 113 °C oil bath temperature. The solid product was then extracted with dry toluene using a Soxhlet apparatus followed by drying under vacuum at 80 °C. The final product was brown in color, and is referred to as CPTS-DZ

(c) Silica gel was functionalized with 2-Mercaptobenzothiazole (MBT) by the Mannich reaction between MBT and γ-aminopropyltiethoxysilane (APTS) modified silica gel. First, 4 g acid washed silica gel was reacted with 100 ml dry toluene and 10 ml APTS, under argon with total reflux at 110°C oil bath temperature for 6 hours. The solid was then filtered and extracted with dry toluene using a Soxhlet apparatus. APTS-Silica was then thermally cured under vacuum at 133°C for 17 hours.

8 g of MBT dissolved in a mixture of 100 ml ethanol and 6 ml formaldehyde solution was reacted with APTS-Silica at 95°C oil bath temperature for 17 hours. The product was then extracted with ethanol using a Soxhelt apparatus, followed by drying under vacuum at 75°C. The final product is called APTS-MBT

D. Adsorbent Characterization

Surface Area and Pore Size Distribution

Nitrogen adsorption-desorption measurements were performed on a Micromeritics Tristar 3000 Porosimeter (Micromeritics Instrument Corporation, Norcross, GA). The adsorption isotherms were used to calculate the BET surface area and pore volume. The average pore diameter was estimated from the mesopore volume and the measured BET surface area following the Gurvitsch approach (Selvam et al., 2001), which is based on the relation: $D_{4V/A} = 4V_P / A$, where V_P is the mesopore volume and A is the specific surface area. The desorption isotherm was used to obtain the pore-size distribution using the BJH method (Rouquerol et al., 1999).

Elemental Analysis

Elemental analysis was used to estimate the density of the active sites on the silica surface. C, H and N wt% were determined using a Perkin Elmer Model 2400 CHN Analyzer (Perkin-Elmer Life and Analytical Sciences, Inc, Boston, MA). High purity helium was used as the carrier gas, while oxygen (99.9%) was used as the combustion gas. The operation temperature was 950°C. S wt% was determined using both Dionex DX-120 ion-chromatography (Dionex Corporation, Sunnyvale, CA) and titration. The titration was performed as follows: the sample was prepared via the United States Pharmacopeia oxygen flask combustion method (United States Pharmacopeia, 1995). Using a microburet, the sample was titrated with sulfate titrant (0.00333 M barium acetate volumetric solution) to a sky blue color with dimethylsulfonazo III indicator solution. Cl wt% was also determined by titration. The sample was dispersed in 10 ml of 1.5% hydrogen peroxide and 40 ml of isopropanol. 0.5 ml of 0.13% diphenylcarbazone in ethanol solution and 1 ml of 0.24 N perchloric acid were then added. The sample was then titrated with 0.003 M mercuric acetate volumetric solution, which has been previously standardized, to a pink endpoint.

Thermo-Gravimetric Analysis (TGA)

The thermal stability of the adsorbents was evaluated using ThermoGravimetric Analysis (TGA) (SDT 2960 Simultaneous DSC-TGA, TA Instruments, New Castle, DE).

The temperature history involved heating the sample at 5°C/min from room temperature to 900°C, and then air cooling to room temperature. The ability of cysteine adsorbent to withstand thermal stresses was evaluated in separate thermal cycling studies. A cycle consisted of heating the adsorbent to 100°C in an oven, maintaining the adsorbent at this temperature for two days, and then allowing it to cool to room temperature, before starting a new temperature cycle.

E. Packed-Bed Evaluations

Nitrogen Oxide Reduction

The reaction setup for the NO removal is shown in Figure 2. The SCR of NO by CO reaction was carried out at atmospheric pressure using a fixed bed Pyrex glass reactor (i.d. 6 mm) containing 0.1 g of catalyst (80-120 mesh) at low temperatures (175–250 °C). Oxygen (Wright Bros., 4.18% in He), carbon monoxide (Matheson, 1% in He) and nitric oxide (Air Products, 2.0% in He) were used as received. The reaction was carried out by varying the NO/CO mole ratios for different O_2 concentrations in the feed and at a space velocity of 50,000 h^{-1}. The reaction temperature was measured by a K type thermocouple inserted directly into the catalyst bed. Prior to the catalytic experiments, the catalyst was activated *in-situ* by passing oxygen for 2 hrs at 673 K. The products were analyzed *on-line* using a Quadrapole mass spectrometer (MKS PPT-RGA) and a chemiluminicence detector.

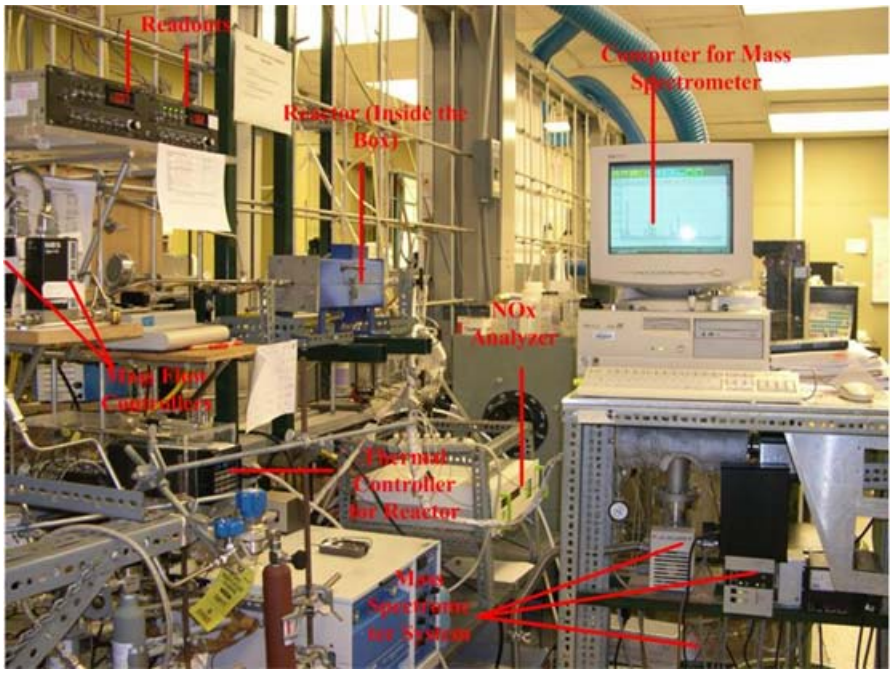

Figure 2. Picture of the SCR Reaction Setup

Mercury Adsorption

The fixed-bed apparatus shown in Figure 3 was used to evaluate mercury uptake by the adsorbents. The assembly consists of a custom-blown glass cell in which a diffusion vial (VICI Metronics, Poulsbo, WA) containing mercuric chloride or a mercury permeation tube is sealed. The cell is immersed in a constant-temperature bath. The cell is connected at both ends to narrower glass tubing which is connected to the rest of the apparatus using PTFE tubing and fittings. Nitrogen (pp. grade) is metered into the mercury generation cell with a mass flow controller. The carrier nitrogen with vaporized mercuric chloride or elemental mercury then passes through an eight-way valve where it mixes with all other metered gases. The flow rates of the individual gases were controlled by Model 1179 Mass Flow Controllers (MFC) connected to models PR4000 and 247D readout/control boxes (MKS Instruments, Andover, MA). One valve of the eight-way valve is plumbed to a glass column (160 mm x 1.5 mm I.D, Ace Glass Inc., Vineland, NJ.) packed with a weighed amount of the adsorbent. The column is placed in a vertical-tubular furnace (5" x 1" ID) with a temperature controller (Model MTF 10/25/130/201, Carbolite, Hope Valley, England), and temperatures up to 1000°C can be achieved.

Effluent from the bed passes through a series of 30 ml midget impingers with coarse fritted cylinders (Chemglass, Vineland, NJ), to measure elemental and oxidized mercury content as per the Ontario Hydro Method (ASTM D6784-02, 2002). This method utilizes a condensation/absorbing system consisting of eight impingers connected in series and immersed in an ice bath. The first, second, and third impingers contain chilled aqueous 1M potassium chloride solution, and are used for collection of oxidized mercury. Elemental mercury is collected in subsequent impingers. The fourth impinger contains an aqueous solution of 5% v/v nitric acid and 10% v/v hydrogen peroxide. The fifth through seventh impingers contain an aqueous solution of 4% w/v potassium permanganate and 10% v/v sulfuric acid. The last impinger contains silica gel or an equivalent desiccant. Each impinger was filled with 25 ml of the absorbing solution. A 1 hour sampling time was used. The amounts of mercuric chloride and elemental mercury captured in the sampling impingers were determined using a cold-vapor atomic absorption analyzer (Buck Scientific Mercury Analyzer, Model 400A, East Norwalk, CT.).

A second outlet from the eight-way valve is used to measure the inlet concentration of mercury or mercuric chloride to the packed bed. It is connected to an identical series of impingers, as described earlier, through a flow restrictor. The volumetric flow rate at the exit was measured with a bubble flow meter. All gas contact surfaces at and downstream of the mercury generator are made from Teflon or glass to ensure inertness toward mercury. Also, all connecting lines downstream of the mercuric chloride vapor generator were heated to approximately 120ºC using heating tape, to prevent vapor condensation. The input stream concentration was measured continuously for three days in order to ensure a constant concentration.

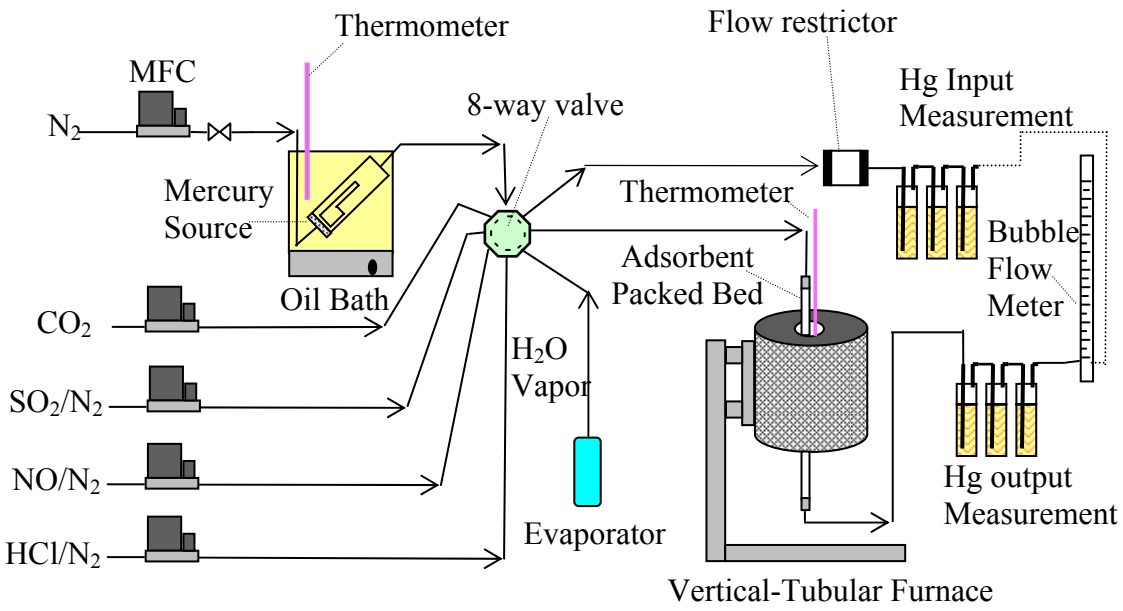

Figure 3. Schematic Diagram of Packed Adsorbent Bed Apparatus

III. Results and Discussion

A. Low Temperature NO_x Reduction with CO

X-ray powder diffraction patterns of titania supported manganese oxide catalysts are shown in Figure 4. The corresponding phase compositions are presented in Table 1. In all the samples, broad diffraction lines due to the anatase phase of titania (JCPDS file no. 21-1272) were observed. No independent lines from crystalline MnO_2 were observed in the XRD patterns, indicating that impregnated manganese oxide is well dispersed on titania support, and it is in amorphous or poorly crystalline state. It can be observed from Figure 4 that the peak intensity of titiania decreased with an increase in manganese content in the catalyst. Measured BET surface areas of the prepared catalysts are presented in Table 1. The specific surface areas of the catalysts are much lower than the pure TiO_2 support. This severe loss in surface area is attributed to blockage of micro pores in the titania support by deposited manganese oxide.

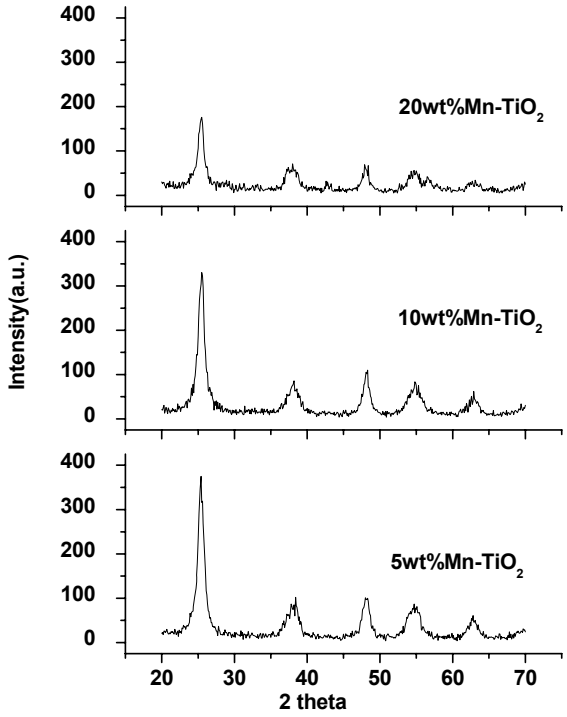

Figure 4. Powder XRD Patterns of the Prepared Catalysts

Table 1. BET Surface Area, Phase Composition and Total Acidity of the Catalysts

Sample	BET surface area (m^2/g)	Phase composition	Total Acidity ($\mu mol\ g^{-1}$)
TiO_2	309	Anatase	-
$5\%MnO_2/TiO_2$	259	Anatase	-
$10\%MnO_2/TiO_2$	236	Anatase	-
$20\%MnO_2/TiO_2$	198	Anatase, MnO_2	23.2

Ammonia TPD was utilized to measure the total acidity of the most active catalyst 20% MnO_2/TiO_2. The total ammonia desorption values are presented in Table 1. This sample showed NH_3 desorption in the 400-700 K range, signifying a broad distribution of surface acid sites. The amount of ammonia desorbed in the case of 20% Mn/TiO_2 sample is 23.2 μmol g^{-1}. The acid sites are distributed in two temperature regions, indicating the presence of two types of adsorbed NH_3 species with different thermal stabilities. The reduction behavior of the 20% MnO_2/TiO_2 catalysts calcined at 673 K was investigated by the Temperature Programmed Reduction (TPR) technique. The TPR pattern of the sample is shown in Figure 5. As can be seen, three prominent reduction peaks were observed for this catalyst at 648, 698 and 763 K. The observed peaks could be attributed to the following sequential reduction of MnO_2. These patterns are consistent with earlier literature reports (Kapteijn et al., 1994).

$$MnO_2 \rightarrow Mn_2O_3 \rightarrow Mn_3O_4 \rightarrow MnO \qquad (1)$$

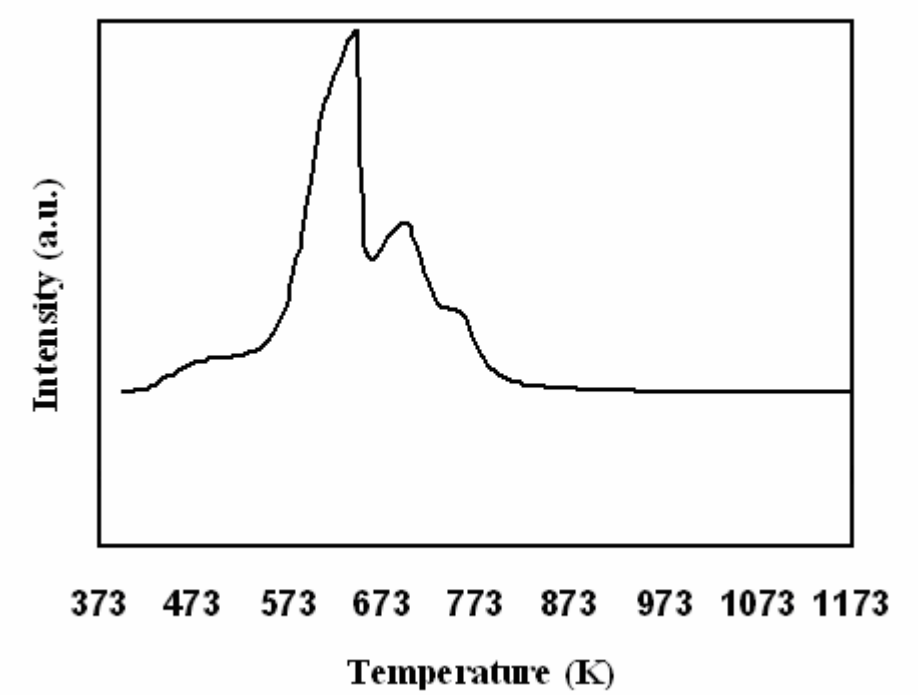

Figure 5. TPR Patterns of the MnO_2/TiO_2 Catalyst

The elementary steps involved in this reaction are shown in the following equations and these are widely accepted in the literature (Xiaoyuan et al., 2004; Byong et al., 1989). Here S denotes the catalyst active site and * denotes activated/adsorbed molecule/atom.

$$CO + S \rightarrow CO^* \qquad (2)$$

$$NO + S \rightarrow NO^* \qquad (3)$$

$$NO^* + S \rightarrow N^* + O^* \quad (4)$$

$$CO^* + O^* \rightarrow CO_2 + 2S \quad (5)$$

$$NO^* + N^* \rightarrow N_2O^* + S \quad (6)$$

$$N_2O^* \rightarrow N2O + S \quad (7)$$

$$N_2O^* \rightarrow N_2 + O^* \quad (8)$$

$$N^* + N^* \rightarrow N_2 + 2S \quad (9)$$

Among the three catalysts studied, the 20% MnO_2/TiO_2 sample showed superior catalytic performance over the others. Catalytic activity results for the SCR of NO with CO at 175 ˚C over 20% MnO_2/TiO_2 sample are shown in Figure 6. This catalyst showed good performance giving more than 65 % NO conversion with 100% N_2 selectivity. Even at the high space velocity (SV) of 50,000 h^{-1} and in the presence of 2 v% H_2O, the catalyst showed excellent performance. This is mainly due to the high surface concentration of manganese and better interaction between anatase support/impregnated oxide, thereby enhancing the redox properties of the catalyst as shown in Figure 5 and Equation 1. All characterization results suggest that moderate acidity, a high surface manganese oxide concentration and redox properties of the catalyst are important factors in achieving better DeNOx performance at low temperature.

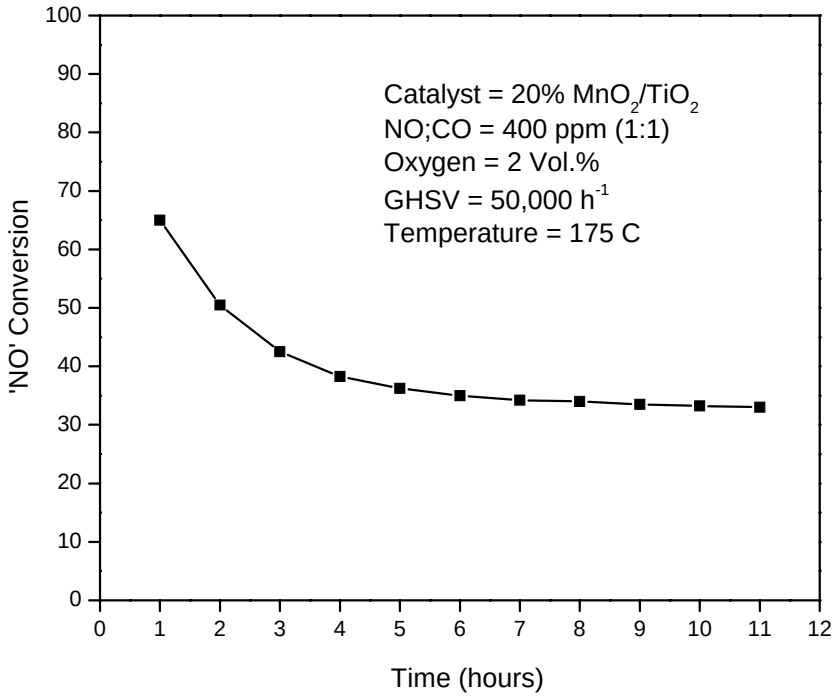

Figure 6. Performance of 20% MnO_2/TiO_2 for SCR of NO with CO at 175˚C.

B. Oxidation of Elemental Mercury

Modification of Chelating Adsorbent

A key objective of this project is to explore the possibility of extending the capability of the subject chelating adsorbent technology to the capture of elemental mercury (Hg^0). In its current form (Abu Daabes and Pinto, 2005), the chelating adsorbent is designed for oxidized mercury. Extension to elemental mercury will make the capture process independent of the metal speciation, and hence of coal type, combustion conditions, plant configuration, etc. The most direct route to achieve this objective is modification of the active nano-layer to incorporate oxidation capacity for elemental mercury. This capability will enable immobilization of elemental mercury by chelation, identical to the path taken by mercury originating from $HgCl_2$. Investigations on the feasibility of this approach have been performed.

Ionic melts are excellent solvents for salts and metals. Salts that have a common ion with the melt are known to have high solubilities in the melt. This is the basis for the high solubility of $HgCl_2$ vapor in the chelating adsorbent. Ionic melts can also be designed to provide strong oxidizing environments. Recently, there has been considerable interest in using room temperature ionic melts as oxidizing media, because of the "green synthesis" potential of this approach. There are a number of successful demonstrations in the literature including the oxidation of benzylic alcohols to carbonyl compounds [Kumar et al., 2004], the oxidation of alkyl and aryl pyridines [Panchgalle et al., 2004], and the oxidation of alcohols to aldehydes [Liu et al., 2003]. Based on these reports, we have conducted preliminary screening experiments to determine the feasibility of oxidizing Hg^0 in ionic melts.

We synthesized a room temperature pyrrolidinium imide molten salt (P_{14}) with 1-butyl, 1-methyl pyrrolidinium cation and bis(trifluoromethane sulfonyl)imide anion [MacFarlane et al., 1999]. This salt was selected because of its stable liquid range, oxidation potential window, and very low volatility. The synthesis procedure is as follows: 6.30g (7.69ml) 1-methyl pyrrolidine (Aldrich) was mixed with 125ml acetonitrile (TEDIA). 12.08g (7.08ml) 1-Iodobutane (Aldrich) was then added dropwise into the pyrrolidine solution in an argon atmosphere. The mixture was stirred overnight at approximately 70°C. The solvent was removed by rotary evaporation, and the solid product was washed with ethyl acetate several times until the filtrate was almost colorless. The final product was dried under vacuum at room temperature for more than 48 hours. This intermediate product (1-n-Butyl-methyl Pyrrolidinium Iodide) is named P_{14}-I, and it is a yellowish solid powder. 1.6g lithium bis(trifluoromethane sulfonyl) imide salt was dissolved into 2g DI water. In another 2g of DI water, 1.27g P_{14}-I was dissolved. These two aqueous solutions were mixed and stirred at room temperature for 3 hours. The product (organic phase) was separated from the aqueous phase by a separation funnel, and was washed with DI water twice to remove any water-soluble impurities. The final product was dried under vacuum at room temperature overnight, and about 2ml of P_{14} was obtained.

The initial evaluation of the P_{14} was done on the apparatus shown schematically in Figure 7. A mercury permeation tube supplied by VICI Metronics (Poulsbo, WA) was used as the source of elemental mercury. The permeation tube is sealed in a U-type glass tube holder and is immersed in a temperature-controlled oil bath. The temperature of the oil bath was fixed at 30°C. N_2 was used as the carrier gas, and the effluent from the U tube was fed to a series of three impingers. The first impinger was filled with P_{14}. The second and third impingers contained KCl and $KMnO_4$, to respectively capture Hg^{2+} and Hg^0 from the effluent of the first impinger. The analysis of these solutions was done by CVAA. By comparing the concentration in the feed and effluent of the first impinger the affinity of P_{14} for Hg^0 was determined.

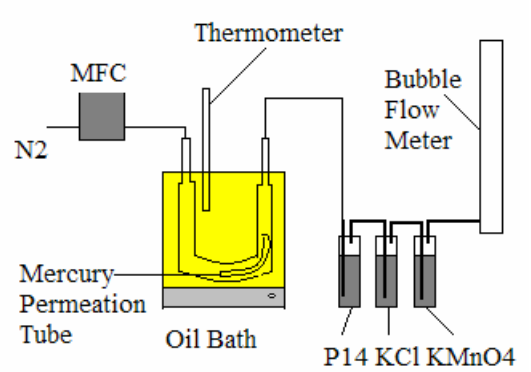

Figure 7. Apparatus for Evaluation of Oxidation Potential of P_{14} for Elemental Mercury

Prior to running tests for Hg^0 uptake by P_{14} ionic liquid, suitable blank experiments were performed to confirm no uptake of mercury by ancillary equipment. When elemental mercury in N_2 was bubbled into the first impinger filled with P_{14} ionic liquid at room temperature, 0.64 µg/h Hg^0 was absorbed, and there was no Hg^{2+} in the effluent (Table 2). We suspect that Hg^0 may be oxidized by the solvent, and the Hg^{2+} forms a complex with P_{14} ionic liquid. In order to confirm this, the same experiment was performed but with 227 ppm HCl added to the carrier gas. Once again 0.64 µg/h Hg^0 disappeared, but 0.63 µg/h of Hg^{2+} was measured in the effluent; i.e., 59% of Hg^0 was oxidized to Hg^{2+} in the P_{14} ionic liquid. In an additional experiment 0.474 g (3mmol) $KMnO_4$ was dissolved in P_{14}, to test for possible enhancements in oxidation capacity. Hg^0 disappeared completely with no Hg^{2+} detected in the effluent.

Table 2. Hg^0 Oxidation Using P_{14} and P_{14}-$KMnO_4$ (Room Temperature).

Experiment	Hg^0 in feed (µg/h)	Hg^0 in effluent (µg/h)	Hg^{2+} in effluent (µg/h)
Impinger with P_{14} -N_2 gas	1.06	0.42	0
Impinger P_{14} -N_2 gas +227 ppm HCl	1.06	0.42	0.63
Impinger P_{14}-$KMnO_4$ -N_2 gas	1.06	0	0

Table 3. Effect of P_{14} Loading on Silica.				
% solvent wt/wt	BET surface area(m^2/g)	Mean pore diameter (nm)	Cumulative pore volume (cm^3/g)	Coating layer Thickness (nm)
0	283	16.3	1.18	0
20	166	16.4	0.81	0.6
25	144	16.0	0.73	0.8
30	130	16.1	0.61	1.0

While these preliminary results are promising, it is recognized that the contacting scheme used is fundamentally different from the proposed LTSCAR. In the latter case uptake will be from the gas to a nano-layer of P_{14} coated on a porous particle or monolith, and the mass transfer rate to the surface of the coating could be a significant issue. Additionally, the bulk liquid tests were conducted at room temperature not at the targeted temperature of 160^0C. It is also essential to determine if P_{14} is a suitable coating for the selected substrate; it should wet the substrate uniformly with a nano-layer without reducing the pore volume and surface area significantly. Preliminary investigations to assess these issues have been conducted. P_{14} was coated on porous silica gel (Grace Davison Grade Number 62). Different amounts of P_{14} were used, and the surface area, pore volume, and pore size were measured (Table 3). Although the pore volume of the P_{14} coated silica decreased monotonically with increases in P_{14} loading, the majority of the high mesopore (>100Å) pore volume remained, which is desired for good flue-gas access to the active surface area. All of the P_{14} coated silicas have a similar pore-size distribution with a defining diameter of 16 nm.

The P_{14} coated silica (25 wt%) was packed in a column and tested for its ability to capture elemental mercury in a fixed-bed at 160^oC. A 6.3 mg sample of the coated silica was used. Shown in Figure 8 is the effluent concentration history for a feed of Hg^0 of 66 ppbv in N_2 at 12 ml/min. The effluent concentration is reported as a fraction of the feed concentration (C/C_0). It is seen that Hg^0 was effectively captured for >40 hours of operation. The total uptake of Hg^0 was 2.7 mg/g of coated silica. It is clear from this un-optimized experiment that the uptake of elemental mercury by the P_{14} nano-coating at the elevated temperature is sufficiently rapid for the contacting scheme envisioned.

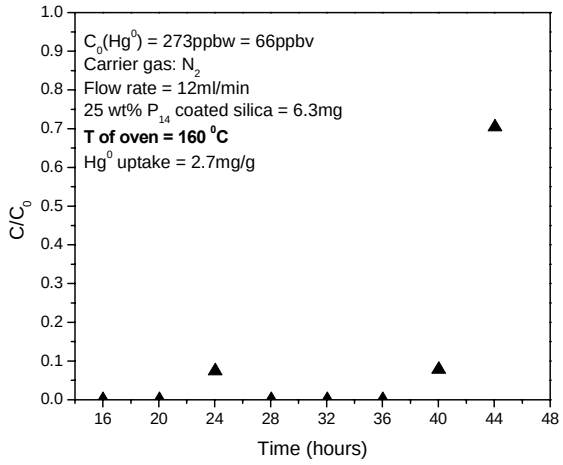

Figure 8. Removal of Hg^0 with 25 wt% P_{14} coated Silica at 160 °C

Titania Supported Hg(0) Oxidizing Catalyst

Another approach to oxidize elemental mercury is to dope titania with manganese. The good redox character of Mn^{3+} and Mn^{4+} (only –0.96 Volts ionization energy) allows

for easy valence changes between the corresponding states of manganese. We have examined the potential of this by doping TiO_2 with controlled amounts of MnO_2, using the procedure described in Section II.A. Specifically, 10% and 20% TiO_2 supported MnO_2 catalysts were tested in a fixed-bed mode on the apparatus shown in Figure 3 (Section II.E), at 175°C and a space velocity of 5000hr^{-1}.

Shown in Figure 9 is the effluent concentration history for Hg^0 removal by the 10% MnO_2/TiO_2 catalyst. Once again, the effluent concentration is reported as a fraction of the feed Hg^0 concentration. The initial experiment was performed with Hg^0 in N_2 carrier gas. The effluent history data for <96 h shows very efficient removal of the Hg^0. It has been reported in Boren et al. (2004) that MnO_2 itself is an oxidizer, it readily exchanges oxygen in a chemical reaction, and it is also well known that MnO_2 has catalytic properties. The authors attribute the oxygen exchange ability to the proton mobility and lattice defects common within most MnO_2 crystal structures. Granite et al. (2000) proposed a reaction mechanism for the oxidation of mercury:

$$Hg_{(g)} + \text{suface} \rightarrow Hg_{(ad)} \quad (10)$$

$$Hg_{(ad)} + M_xO_y \rightarrow HgO_{(ad)} + M_xO_{y-1} \quad (11)$$

$$HgO_{(ad)} + M_xO_{y-1} + 1/2O_{2(g)} \rightarrow HgO_{(ad)} + M_xO_y \quad (12)$$

$$HgO_{(ad)} + M_xO_y \rightarrow HgM_xO_{y+1} \quad (13)$$

The fist step is the adsorption of elemental mercury onto the surface of MnO_2. The adsorbed elemental mercury is then oxidized to mercuric oxide through the reduction of MnO_2. If oxygen is present (though it is not necessarily required), the reduced manganese oxide is re-oxidized, and the mercuric oxide reacts with this oxide to form a binary oxide. It is noted that TiO_2 support does not exhibit activity for elemental mercury Zhuang et al. (2000).

The possible interference of water vapor with Hg^0 oxidation/removal by the catalyst was also studied. 7% (v/v) water vapor was introduced into the system, as shown in Figure 9 (<96 h). Essentially no effect is observed on the effluent concentration history.

The effect of SO_2 on catalyst performance was determined by introducing SO_2 at 200 ppm into an Hg^0–N_2 stream (water free) that had been contacting the catalyst for 96 h (Figure 9). Almost an immediate increase in the Hg^0 concentration in the effluent was observed. Upon switching off the SO_2 (≈ 156 h), the catalyst appears to recover some of its activity, but not to the activity level before the introduction of SO_2.

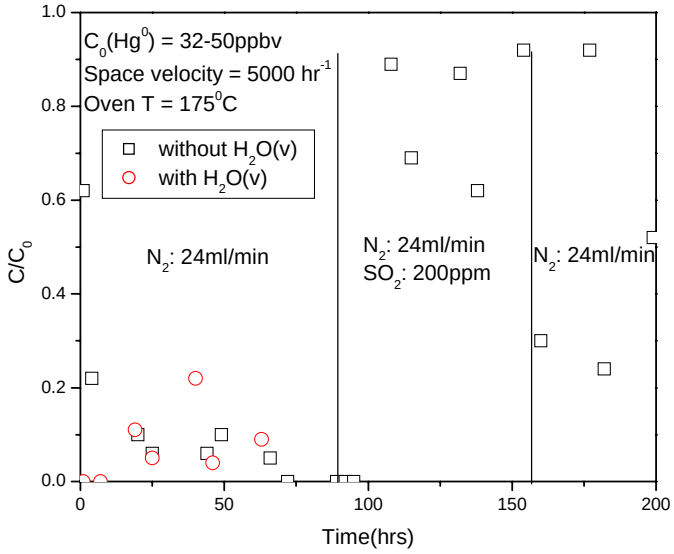

Figure 9. Effluent Concentration History of Hg^0 from 10% MnO_2/TiO_2 Bed

The effect of MnO_2 loading on Hg^0 oxidation/removal was investigated by performing an experiment with 20% MnO_2/TiO_2 catalyst. As shown in Figure 10, the performance of this catalyst is essentially identical to 10% MnO_2/TiO_2. Thus, increasing the metal loading beyond 10% is not expected to improve effectiveness.

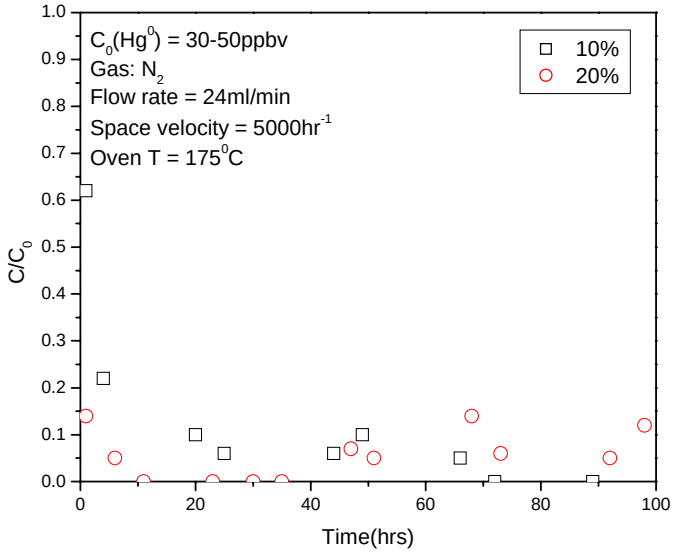

Figure 10. Effect of MnO_2 Loading on Effluent Concentration History of Hg^0

We have also investigated Hg^0 oxidation/removal with 20% MnO_2/TiO_2 catalyst that had previously been used for NO reduction. The purpose of this experiment was to test the potential of this catalyst to simultaneously remove Hg^0 and reduce NO. Shown in

Figure 11 is the effluent concentration of Hg^0 from this catalyst bed. It is observed that Hg^0 was effectively removed by the catalyst for the entire duration of the experiment (80 h). This suggests that the catalyst will have the potential to simultaneously act as an oxidizing catalyst for Hg^0 and a reducing catalyst for NO. An evaluation for simultaneous removal with a feed containing both Hg^0 and NO is planned for Phase II of this project.

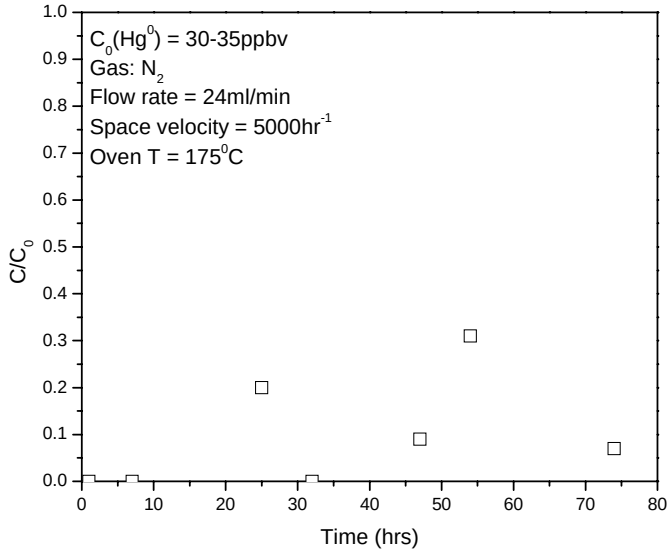

Figure 11. Hg^0 Effluent Concentration History for Packed Bed of 20% MnO_2/TiO_2 Catalyst Previously Used for NO Reduction

C. Thermally Robust Adsorbents for Oxidized Mercury

The synthesis procedures for the three silica-based adsorbents designed to operate at higher temperature (160°C), mercaptopropyltrimethoxysilane (MPTS), Dithizone (CPTS-DZ) and Mercaptobenzothiazole (APTS-MBT), are described earlier in Section II.C. In this section we present results from experiments to evaluate the properties of these materials. All three materials were studied for their thermal stability and specific pore volume and surface area. Based on these results, the most promising (MPTS) was evaluated for its ability to capture oxidized mercury in a fixed-bed.

MPTS Adsorbent

TGA was performed on the MPTS adsorbent as described earlier (Section II.D). The results are shown in Figure 12. About 8.5 wt% of the adsorbent was lost in the process of heating to 900°C. This loss corresponds to both surface-water release and MPTS decomposition. The water release is calculated to account 3.9% of the total loss, based on experiments with un-activated silica (not shown here). Therefore, the net loss due to MPTS degradation is 4.6%. The derivative curve in Figure 12 shows that thermal decomposition of MPTS bonded to silica surface occurs in two steps. The first is between 200 and 420°C with a total weight loss of ~3.4%. The second peak appears in the range

of 420-650°C with a total weight loss of 2.8%, including 1.1% due to water release from condensation of surface silanol groups (obtained from separate baseline experiments).

The effects of longer-term exposures to high temperatures on the active sites of MPTS adsorbent were determined to establish its upper operating limit. Two samples were held isothermally at 220°C and 250°C in an oven for 24 hours each, and then subjected to elemental analysis (samples MPTS-220°C and MPTS-250°C, respectively, in Table 4). The results show that heating the MPTS adsorbent at 220°C for 24 hours caused ≈37% reduction in S wt%, while heating to 250°C caused ≈69% reduction. Since the TGA results show a rapid loss of weight starting at 200°C, the combined results suggest that the decomposition of the thiol (–SH) active groups starts at this temperature. Thus, it is concluded that the MPTS adsorbent is thermally stable up to 200°C.

Table 4. Elemental Analyses of MPTS Adsorbent Before and After Exposure to Elevated Temperatures (24 h).

Sample	Element wt%		Surface Coverage ($\mu mol/m^2$)
	C	S	
MPTS-R.T.	3.08	1.87	2.12
MPTS-220°C	2.2	1.17	1.32 (*37% loss*)
MPTS-250°C	1.51	0.58	0.66 (*69% loss*)

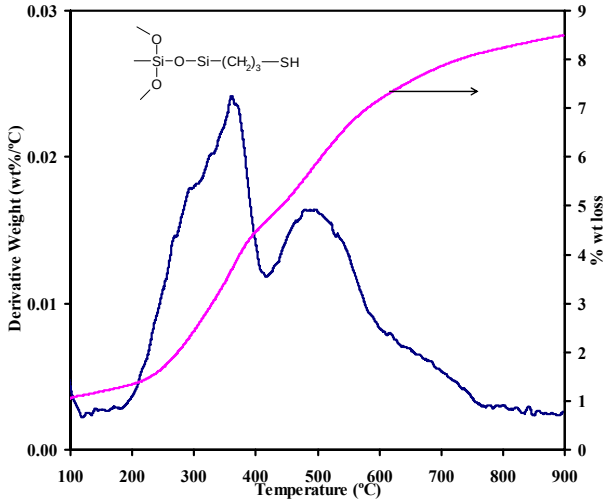

Figure 12. TGA Weight Loss and Derivative Weight Loss for MPTS Adsorbent

CPTS-DZ Adsorbent

TGA was performed on CPTS-DZ adsorbent using the procedure described in Section II.D, to establish the upper temperature limit for the adsorbent. Figure 13 shows the % weight loss and the derivative curves for both CPTS-Silica (the first step of the activation process is to link CPTS to the surface) and for the fully functionalized adsorbent (CPTS-DZ). For CPTS-Silica, the total weight loss was 8.16%, which corresponds to both water and CPTS release from the silica surface. Characterization of the silica substrate showed that total surface-water release was 3.95 wt%, including

physical and chemically bonded water. Therefore the net loss due to CPTS is estimated to be only 4.21%. The derivative curve for CPTS shows three different desorption peaks, the first from 170-300°C, the second from 300-500°C, and the third from 500-700°C. These peaks correspond to the progressive release of different fractions of CPTS from the silica surface.

For the fully functionalized adsorbent (CPTS-DZ), the total weight loss up to 900°C was 12.15%, with only 4% corresponding to the release of immobilized DZ molecules (Figure 13). The derivative curve for CPTS-DZ shows three desorption peaks in the range of 140-225°C, 225-290°C, and 290-600°C, with a corresponding loss of 20%, 50%, and 75% of total DZ bonded to silica surface, respectively.

The effect of longer-term exposure to high temperatures was evaluated by holding the CPTS-DZ adsorbent isothermally in an oven at 180°C for 24 hours followed by elemental analysis (Table 5). The results showed that the adsorbent lost approximately 23% of its active sites if operated at 180°C in a continuous mode, i.e., fixed-bed mode. However, the highest flue-gas temperature out of the particulate collector is 160°C. Therefore, CPTS-DZ adsorbent is expected to operate satisfactorily at the temperatures of flue-gas out of particular collectors without the need for pre-cooling of flue-gas, and with no significant loss of the CPTS-DZ active sites.

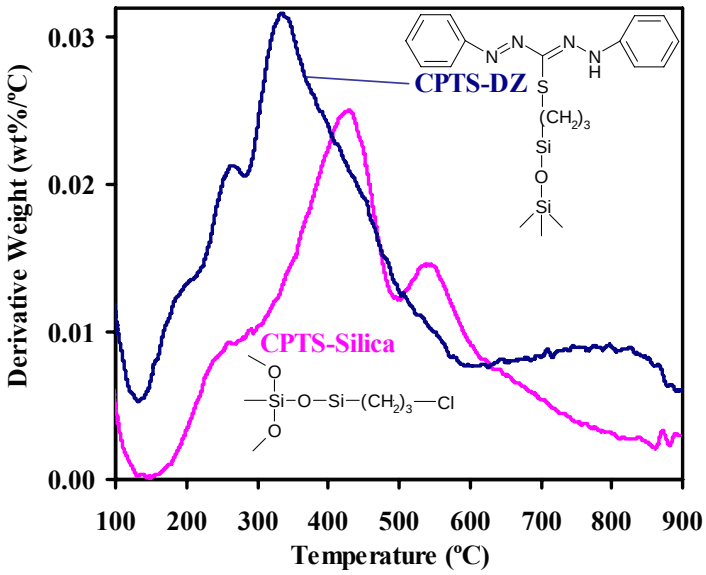

Figure 13. TGA Derivative Weight Loss for CPTS-DZ Adsorbent at Different Stages of the Synthesis

Table 5. Elemental Analysis of CPTS-DZ Adsorbent Before and After Exposure to Elevated Temperature (24 h).		
Sample	N wt%	Surface Coverage ($\mu mol/m^2$)
CPTS-DZ-R.T.	0.97	0.58
CPTS-DZ-180°C	0.75	0.45 *(23% loss)*

APTS-MBT Adsorbent

Identically to the other adsorbents TGA was performed on APTS-MBT using the procedure described in Section II.D. Figure 14 shows the derivative weight loss curves for APTS-Silica (first step in functionalization process) and for APTS-MBT (fully functionalized adsorbent). The weight loss curves (not shown) indicate degradation above approximately 190°C for both APST-Silica and APTS-MBT, indicating that the linking APTS is unstable above this temperature. The approximate upper temperature limit from TGA for APTS-MBT adsorbent was verified by placing two samples in an oven at 190°C and 250°C for 24 hours each. Comparison of S wt% before and after heating (Table 6) showed a 14% loss in S at 190°C and a 58% loss at 250°C. Thus, the upper thermal stability of APTS-MBT adsorbent is estimated to be 190°C.

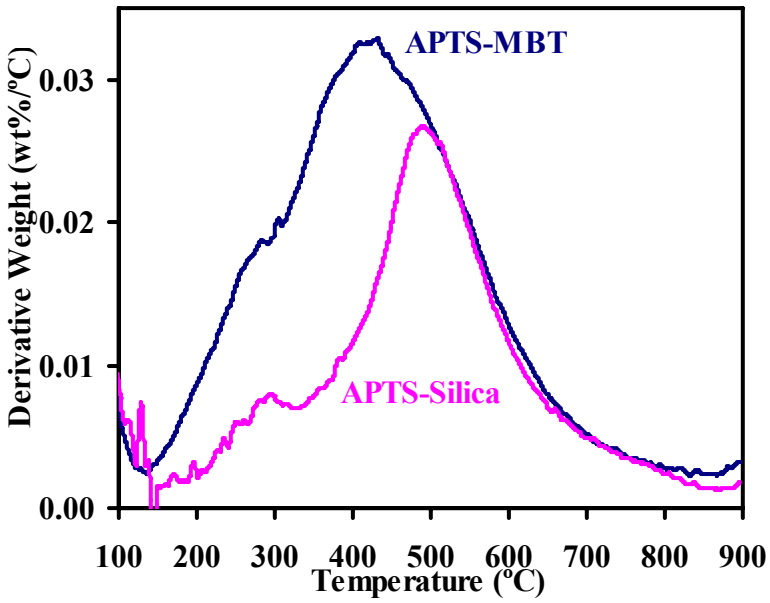

Figure 14. TGA Derivative Weight Loss for APTS-MBT Adsorbent at Different Stages of the Synthesis

Table 6. Elemental Analyses of APTS-MBT Adsorbent Before and After Exposure to Elevated Temperatures (2h h).		
Sample	S wt%	Surface Coverage ($\mu mol/m^2$)
APTS-MBT-R.T.	1.39	0.76
APTS-MBT-190°C	1.2	0.65 *(14% loss)*
APTS-MBT-250°C	0.58	0.31 *(59% loss)*

Table 7 compares the characteristics of the three thermally robust chelating adsorbents developed in this project relative to the prototype (cysteine) that was available prior to this work. The operating temperature limits are well above the targeted minimum of 160°C. Also reported in Table 7 are the BET specific surface areas, the average pore diameter and the cumulative specific pore volume. Figures 15 and 16 show the detailed pore-size distribution and cumulative pore-volume plots, respectively. It is noted that while all versions of the adsorbent have high specific area and volume, these correlate with the size of the attached ligand; the larger the ligand the smaller the available pore volume and surface area.

Table 7. Comparison of the Characteristics of Chelating Adsorbents					
Adsorbent	Structure of Ligand	BET Area (m^2/g)	Average Pore Diameter (nm)	Cumulative Pore Volume (cm^3/g)	Thermal Stability T_{upper} (°C)
Silica Substrate		283	16.0	1.18	-
Silica with 3-mercaptopropyltrimethoxy-silane (MPTS)	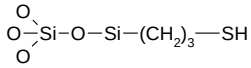	259	15.7	1.02	200
Silica with Dithizone (CPTS-DZ)	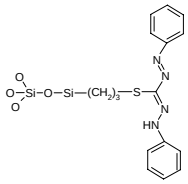	215	15.3	0.82	180
Silica with 2-Mercaptobenzothiazole (APTS-MBT)	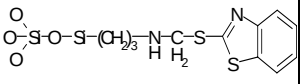	245	13.6	0.83	190
Silica with Cysteine (prototype)	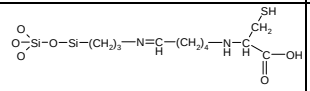	235	11.6	0.75	135

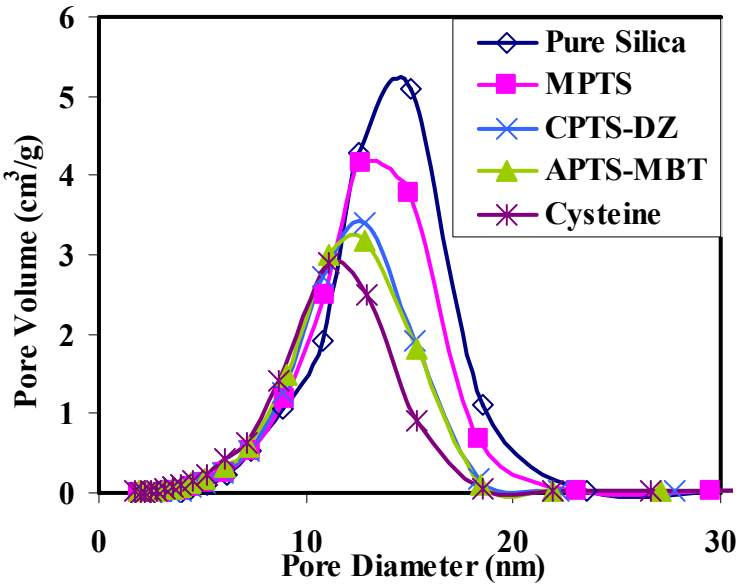

Figure 15. Pore-Size Distributions of Thermally Robust Chelating Adsorbents Compared to Cysteine Prototype and Pure Silica Substrate

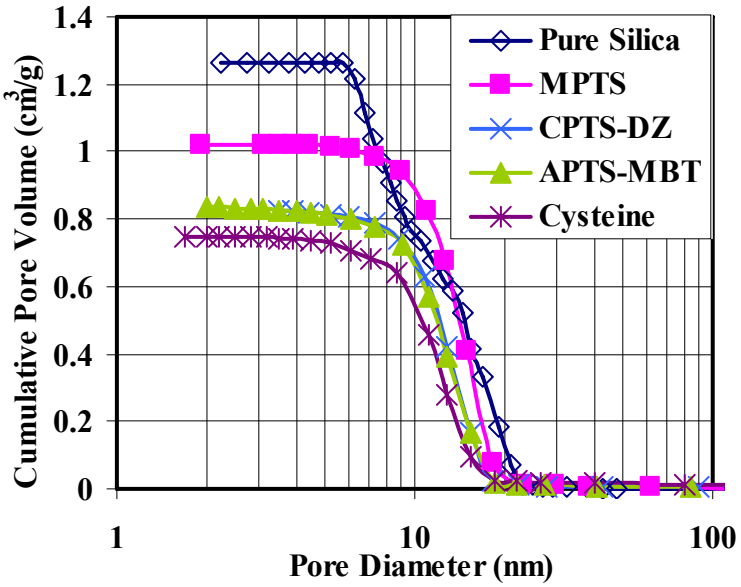

Figure 16. Cumulative Pore Volumes of Thermally Robust Chelating Adsorbents Compared to Cysteine and Pure Silica Substrate

Based on these results, it was concluded that the MPTS adsorbent is most promising. It has the highest thermal stability limit (200°C) of the adsorbents synthesized, well above the targeted temperature of 160°C. The relatively small size of the ligand results in an activated adsorbent that has a characteristic pore diameter that is only marginally smaller (15.7 Å) than that of the starting substrate (16 Å). Additionally, the

specific pore volume and surface area are the highest of the functionalized adsorbents. Finally, and most importantly, the activation process results in ligand densities of MPTS on the surface (2.1 μmol/m^2) that are substantially higher than for the other adsorbents, and suggest very high adsorption capacities for mercury.

Operating Capacity Evaluations

In order to fully activate the MPTS adsorbent, it is necessary to coat the surface with a noanolayer of ionic solvent. The ionic solvent Methylpolyoxyethylene(15)octadecanammonium chloride (MEC) was used. The procedure for coating the surface is identical to that described earlier (Abu Daabes and Pinto, 2005). It was reported in that paper that the thermal stability of MEC on the silica surface is substantially higher (>300^{o}C) than that of the chelating ligand.

Table 8 shows the structural characteristics of four different silica substrates used in the packed-bed evaluations of the MPTS adsorbent. The particle sizes shown were measured by a laser scattering particle size distribution analyzer (Malvern Mastersizer S series). All the starting substrates have similar particle sizes, except for Grade #646, which has a larger particle size, with a size range of 250-500μm.

Table 8. Characteristics of Si-M-M Adsorbent Relative to Starting Substrate

Silica Substrate Grade #	Particle Size (μm)	Pore Size (Å)		BET Surface Area (m^2/g)		Pore Volume (cm^3/g)	
		Substrate	Si-M-M	Substrate	Si-M-M	Substrate	Si-M-M
62	75-250	163	157	283	143	1.18	0.56
646	250-500	163	165	311	140	1.18	0.59
22	75-250	78	79	461	147	0.98	0.38
sp-540-10232	100-300	700	693	84	43	0.59	0.49

Pore sizes of the starting silica substrate and the fully functionalized adsorbent, Silica-MPTS-MEC (Si-M-M), are compared in Table 8. It can be seen that for all four pore sizes, activation does not result in a significant reduction in pore size. However, the specific pore area and pore volume are reduced by approximately 50%. This in conjunction with the MPTS result in Table 7 (MPTS adsorbent not coated with MEC) suggests that the loss in pore volume and surface area is due to partial pore blockage by the MEC.

$HgCl_2$ dynamic adsorption experiments were performed on Si-M-M adsorbents of Table 8 using the apparatus and procedure described in Section II.E. A simulated flue gas (CO_2: 16%, HCl: 150ppm, SO_2: 1500ppm, NO: 500ppm, H_2O (v): 6%, N_2: balance) at 160°C was fed at 100 ml/min (≈ 1 m/s). Figure 17 shows the performance of Grade # 646 Si-M-M in a typical long-term fixed-bed adsorption. The simulated flue gas contained 12

ppbv $HgCl_2$. The results are reported as the ratio of effluent $HgCl_2$ concentration (C) to the corresponding feed concentration (C_o). It is seen that the mercury is effectively captured at very high capacity; the uptake was ≈58 mg Hg/g adsorbent, and this value is a lower bound on the mercury capacity, since mercury breakthrough was not observed at the end of 32 days of continuous operation. Based on the elemental analysis (Table 4) the adsorbent is estimated to have a capacity of 117 mg/g.

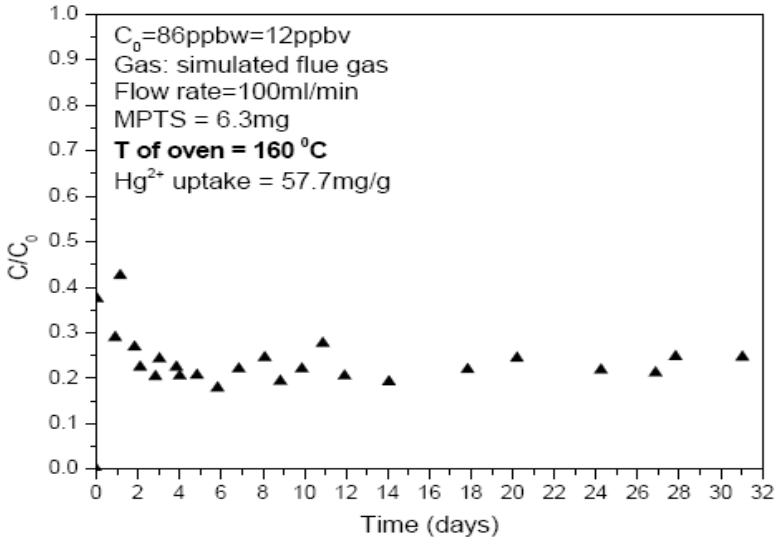

Figure 17. Fixed-Bed Adsorption of $HgCl_2$ on Grade # 646 Si-M-M (250-500 µm, 150 Å) at 160°C

Figure 18 shows the fixed-bed adsorption performance for adsorbents of different particle sizes; it can be seen that larger particle sizes are associated with reduced mercury capture effectiveness, though overall capture efficiency is high for all cases.

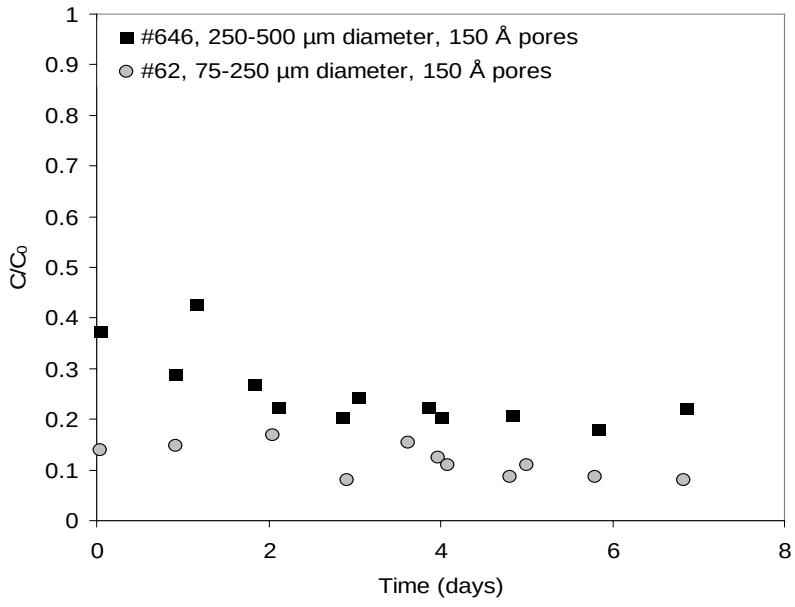

Figure 18. Effect of Particle Size on Fixed-Bed Adsorption of HgCl2 from Simulated Flue Gas Using Si-M-M Adsorbent. T=160°C.

The effect of particle **pore** size on Hg uptake was also evaluated. Figure 19 shows the performance of three fixed beds of MPTS adsorbent of similar particle size and varying pore sizes (60 - 500 Å) at operating

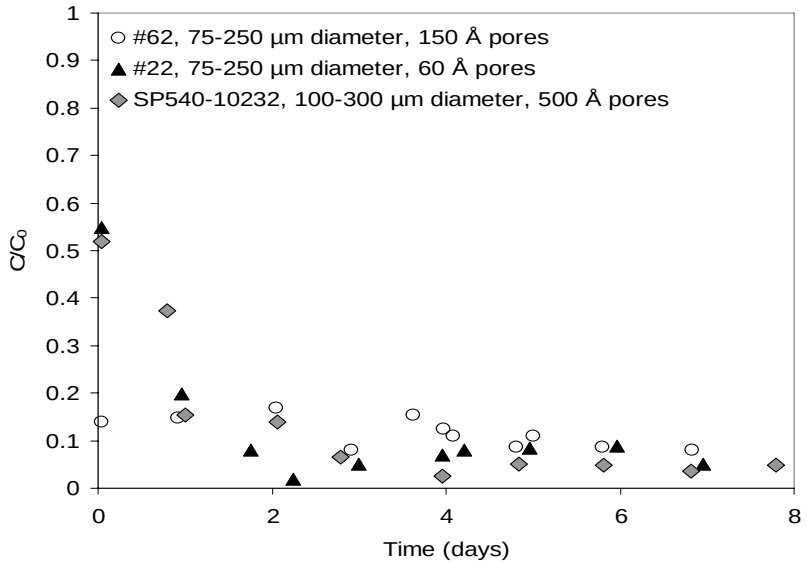

conditions similar to those described above. Following the usual initial transition, the column stabilizes at a very low C/C_0 value, indicating that with proper selection of pore diameter and particle size very efficient removal of Hg^{2+} is possible.

Figure 19. Effect of Pore Size on Fixed-Bed Adsorption of $HgCl_2$ from Simulated Flue Gas Using Si-M-M Adsorbent. T=160°C.

IV. Preliminary Assessment of Economic Impact

Low temperature SCR catalysts offer the opportunity to remove NO_x without the need to reheat the flue gas stream, with obvious economic benefits. The use of CO as a reductant is a novel concept, and if proven successful will have significant socio-economic and environmental benefits. It will substitute the current reductants for medium and low temperature SCR, namely ammonia and/or urea, an upgrade for the industry with tremendous benefits. It will eliminate the need to buy reductants and transport them through populated areas, it will minimize equipment corrosion, and eliminate storage of reductants. Also, the operating cost can be expected to decrease significantly. It is estimated, assuming a 1:1 molar ratio requirement of CO:NO (based on results in Figure 6) and 70 wt% carbon content in coal, that the weight of coal required to generate sufficient CO will be approximately equal to the weight of NH_3 for the same duty. This will translate into a significant operational cost savings, since the cost of anhydrous ammonia (≈$330/ton in the Midwest) is substantially higher than that for coal (≈$50-60/ton). The use of CO as a reductant is also likely to be more acceptable, in comparison to the N-based reductants, to citizens residing close to utilities. Of course, this will be the case only if Pt-based CO oxidation catalysts are placed at the exit of the clean-up train, to ensure that unreacted CO does not enter the atmosphere (Pt on conventional supports are excellent, inexpensive and easy to install catalysts for CO oxidation to CO_2). The necessary amount of CO will be produced on-site by partially burning/oxidizing a small amount of coal (≈0.5% of the coal charged to the boiler). The generated CO will be distributed into the SCR reactor with the same distribution system used for ammonia, thus keeping this cost the same. Needless to say, the production of CO

will be directly related and follow the need to treat NO_x emissions. Another significant advantage of CO is that in case of slippage solid byproducts such as ammonium sulfate and ammonium bisulfate will not be formed; these result when escaped ammonia and sulfur dioxide react under certain conditions.

The incorporation of concomitant mercury removal in the SCR unit has the potential for reducing the total cost of environmental compliance, and incorporates the significant advantage of a smaller retrofit imprint for existing plants. Additionally the availability of a high capacity, selective adsorbent with strong binding energy for mercury has the added advantages of reducing secondary waste and providing tighter control on the ultimate fate of the captured mercury. However, the greatest potential benefit appears to be in the much lower cost for capture, as described below in an estimate for a full-scale power plant.

While it is recognized that a cost estimate at this stage is preliminary, particularly since the contacting configuration has not been defined, it is an important early indicator for feasibility. As a basis, the estimate is for a 13000 MW plant, assumes an emission factor of 20 μg/dscm for mercury [McDermott, 1999], and a moisture content in the flue of 1.082 moles wet flue/mole dry flue [Stultz, 1978]. It is estimated that the volumetric flow of flue gas for this plant at 245°F is 3590 acfm/MW [Stultz 1978].

The amount of adsorbent required depends on the operating capacity. An operating capacity of 12 mg Hg/g adsorbent was used; this is a very conservative estimate based on the observed operating capacity of 58 mg Hg/g adsorbent obtained experimentally (Figure 17).

Shown in Table 9 is the estimated mass of adsorbent required to capture all the mercury emitted from the 1300 MW plant burning a blend of Ohio 5,6 & 7 coal [McDermott, 1999] for one year. This estimate, 75.8 metric tons, represents a very small adsorbent requirement relative to the amount of activated carbon in the duct injection process. For the same situation, based on estimates in the literature [US EPA, 1999], the activated carbon requirement is in the range 5500 -13500 metric tons per year.

Table 9. Characteristics of Adsorbent Bed with 1-Year Capacity for Mercury

Time of Operation (days)	365
Capture Requirement (%)	100
Mass of adsorbent (metric tons)	75.8
Volume of adsorbent (m^3)*	57
Flue Gas Velocity (m/min)	16
Adsorbent Bed Thickness (cm)**	1.4

*Packing density = 0.6; Density of adsorbent = 2.2 g/cm^3
** 50% bed utilization assumed (152 metric tons of adsorbent)

The small adsorbent inventory (57 m^3/year) is very desirable. The small ratio of adsorbent volume/flue-gas volume eliminates the need for regeneration, and imposes a relatively small added pressure drop in the flow stream. For the 1300 MW plant, and using a flue-gas design velocity of 16 m/min, an adsorbent bed thickness of only 1.4 cm is required; this incorporates a 100% over-design to minimize pollutant leakage. This means that with the proper selection of particle size (≥500μm), the system

can be designed to impose a pressure drop of less than 1.25 in. of water on the flow stream.

A cost analysis to estimate target prices for the chelating adsorbent, at selected levels of total mercury removal cost, was performed. The equipment estimate is for a fixed-bed adsorber. This was used *in lieu* of the LTSCAR, because cost data do not exist for the latter. It is recognized that the cost estimate is conservative, since integration of NO_x and Hg in a LTSCAR is expected to substantially reduce capital expenditure relative to the installation of separate control units for each pollutant. The capital cost estimate for the adsorber is based on packaged, custom, automatic systems for commercial and industrial-scale units of the same size (300,000 lb adsorbent). The size selected is for 1 year of continuous operation (no recharge or regeneration) on the 1300 MW plant, with a 100% over-design on the amount of adsorbent required.

Shown in Table 10 are target adsorbent prices that would have to be achieved for various scenarios: (1) a total removal cost of $30,000/lb Hg, which is the lowest cost projected by DOE with existing technology [Figueroa, 2003]; (2) a total removal cost of $8000/lb Hg, which is the projected estimate for the new Sorbent Technology adsorbent [Nelson, 2003]; (3) a total removal cost of $3000/lb Hg, which represents an order of magnitude reduction in cost over the lowest current cost; and (4) a target cost of $1000/ lb Hg removed.

To put the target prices in perspective, it currently costs $31/lb to make the adsorbent in our laboratory, using materials bought in small quantities at expensive research supplier prices. It is anticipated, based on the price structure for commercial, specialty adsorbents, that a price target of $3-5/lb can be easily achieved. Thus, we are optimistic that this approach will achieve the goal of reducing the cost of mercury capture by at least an order of magnitude over the activated carbon injection process.

Table 10. Estimates of Target Adsorbent Price versus Removal Cost

Total Cost for Removal of Mercury ($/lb Hg removed)	Installed Adsorber* + Labor# + Maintenance+ + Power ψ + Overhead℘ ($/lb Hg removed)	Cost for Adsorbent ($/lb Hg removed)	Target Price for Adsorbent ($/lb adsorbent)
30,000	500	29,500	176
8,000	500	7,500	45
3,000	500	2,500	15
1,000	500	500	3

*300,000 lb unit with instrumentation & controls; installation cost 40% of Purchase Price (PP); indirect cost 45% of PP; 10 year straight-line depreciation; #8760 hours/year; $20/hr; 15% supervisory charge; +5% of total capital cost; ψ5¢/kwh; ℘60% of labor + maintenance

V. Conclusions

A preliminary study of the feasibility of the LTSCAR process for the simultaneous removal of NO_x and mercury from the flue gas of coal-fired power plants has been completed. This study investigated the possibility of using carbon monoxide as a reductant for NO_x at low temperature with a titania supported manganese dioxide catalyst. Additionally, the development of a chelating adsorbent for the simultaneous removal of both oxidized and elemental mercury was pursued. Based on the results of this study, the following major conclusions were reached:

- It is possible to reduce NO_x to N_2 at high conversion and selectivity using CO over a titania supported MnO_2 catalyst at low temperature (175^0C).

- Chelating adsorbents for oxidized mercury can be developed with stability for extended operation at the desired temperatures (< 200^0C). These adsorbents have been shown to have very high operating capacities for oxidized mercury (at least 58 mg/g adsorbent at 160 ^{0}C).

- It is possible to capture elemental mercury on the chelating adsorbent through inclusion of a mercury oxidation step either *in situ* or separately on a titania supported MnO_2 catalyst. Additional work is required to improve performance in both cases.

- Preliminary analyses of the benefits of the proposed LTSCAR approach suggest significant potential economic and environmental advantages.

Based on the promising results of this project, a Phase II project has been approved by DOE and is currently in progress. The follow-up effort will focus on fundamental and applied research to further develop the catalysts and adsorbents from Phase I. Bi- and tri-metallic titania supported catalysts will be synthesized for low temperature NO_x removal using CO as the reductant. Targeted characteristics will be operation in the 140-160^{o}C range with complete transformation of NO_x to N_2, time stability, durability and low cost. Particular emphasis will be placed on achieving extended tolerance to SO_2 and H_2O at expected flue gas concentrations. In parallel, a high capacity chelating adsorbent for mercury will be developed for use in the LTSCAR. The adsorbent will achieve the removal of both elemental and oxidized mercury. Porous silica substrates will be used to support an engineered nano adsorbent layer that can oxidize elemental mercury and strongly and selectively bind the oxidized mercury through chelation. The influence of the adsorbent, catalyst and reductant on mercury speciation will also be evaluated. The effectiveness of the catalyst and the adsorbent will be determined separately and in combination in a simulated flue-gas flow system.

VI. References

Abu Daabes, M. and N.G. Pinto, *Chem. Eng. Sci*., **60**(7), 1901-1910 (2005).

Boren R.M., C.F. Hammel, M.R. Bleckinger, *Proceedings of ASME POWER*, 515-523 (2004).

Byong, K.C., H. S. Brent, E. B.James, *J. Catal.* **115**, 486 (1989).

Figueroa, J., "Update on USDOE Hg Programs and Opportunities," Paper presented at OCDO Ohio Mercury Forum, Columbus, Ohio, April 18, 2003.

Granite, E.J., H.W. Pennline and R.A. Hargis, *Ind. Eng. Chem. Res*. **39**, 1020-1029 (2000).

Kapteijn, F., L. Singoredjo, A. Andreini, *Appl. Catal. B*, **3**, 173 (1994).

Kumar, A., N. Jain and S.M.S. Chauhan, *Synthetic Communications*, **34**(15), 2835-2842 (2004).

Liu, Z. Z.-C Chen and Q.C. Zheng, *Org. Lett.,* **5**(18), 3321 (2003).

MacFarlane, D.R., P.Meakin, J.Sun, N. Amini and M. Forsyth, *J. Phys. Chem. B,* **103**, 4164-4170 (1999).

McDermott Technology Inc, Advanced Emissions Control Development Program. Phase III, Final Report to DOE, OCDO, ODD and Babcock & Wilcox, Alliance Ohio (1999).

Nelson Jr., S., "Coal–Fired Mercury in Ohio and Control Testing at an Ohio Site," Paper presented at OCDO Ohio Mercury Forum, Columbus, Ohio, April 18, 2003.

Panchgalle, S.P., S.M. Choudhary, S.P. Chavan and U.R. Kalkote, *J. Chem Res.,*Aug., 550-551 (2004).

Rouquerol, F., J. Rouquerol and K.Sing, Adsorption by Powders & Porous Solids: Principles, Methodology and Applications. Academic Press, San Diego, CA (1999).

Selvam, P., S.K. Bhatia and C.G. Sonwane, *Ind. Eng. Chem. Res.*, **40**, 3237-326 (2001).

Stultz, S.C. and J.B. Kitto., eds. "Steam: Its Generation and Use," 40th edition, The Babcock & Wilcox Company, Barberton, OH (1978).

United States Phramacopeia, The National Formulary, (1995). Method 471, Oxygen flask combustion, USP 23, NF18. The United States Pharmacopeial Convention, Inc., Rockville, MD, 1748.

US EPA, Analysis of Emission Reduction Options for the Electric Power Industry, Office of Air and Radiation, March (1999).

Xiaoyuan, J., D. Guanghui, L. Liping, C. Yingxu, Z. Xiaoming, *J. Mol. Catal. A*, **218**,187 (2004).

Zhuang Y., P. Biswas, M.E. Quintan, T.G. Lee, E. Arar, *Proceedings of the Air and Waste Management Association 93rd Annual Meeting and Exhibition,* 331 (2000)